Energy & Environmental Science

Accepted Manuscript

ROYAL SOCIETY OF CHEMISTRY

www.rsc.org/ees

Tetrathiafulvalene derivative (TTF-1) was introduced to perovskite solar cells as dopant-free hole-transporting material, yielding an efficiency over 11%.

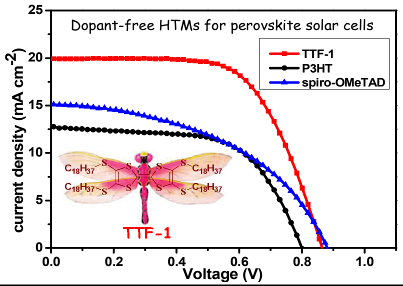

Energy &

Environmental Science

RSCPublishing

COMMUNICATION

Dopant-free Hole-Transporting Material for Efficient and Stable Perovskite Solar Cells

Cite this: DOI: 10.1039/x0xx00000x

Jian Liu, Yongzhen Wu, Chuanjiang Qin, Xudong Yang,* Takeshi Yasuda, Ashraful Islam, Kun Zhang, Wenqin Peng, Wei Chen and Liyuan Han*

Received 00th January 2012,
Accepted 00th January 2012

DOI: 10.1039/x0xx00000x

www.rsc.org/

An efficient pristine hole-transporting material (HTM), tetrathiafulvalene derivative (TTF-1) was introduced to perovskite solar cells, without use of p-type dopants. As compared to cells based on well-known p-type doping spiro-OMeTAD, perovskite solar cells based on dopant-free TTF-1 performed a comparable efficiency of 11.03%; moreover, the stability of dopant-free TTF-1 based cell was greatly improved by 2 fold in air at a relative humidity of ~40%. To the best of our knowledge, this is the first case of perovskite solar cells employing dopant-free HTM based on tetrathiafulvalene derivative yielding an efficiency over 11%. The present finding paves a way for development of efficient dopant-free HTMs for perovskite solar cells, which promote the advancement of cost-effective and practical perovskite solar cells.

Organometal halide perovskites have received increasing attention beginning with their incorporation as sensitizers into dye-sensitized solar cells by Miyasaka et al. in 2009.[1] Very recently, significant progress has been realized in solid-state inorganic-organic hybrid perovskite solar cells,[2,3] with high efficiency over 15%,[4-6] attracting tremendous attention in the field of photovoltaics.[7-11] The light harvesters ABX_3 (A = CH_3NH_3 or $NHCHNH_3$, B = Pb, and X = Br, Cl, or I) have been demonstrated to possess several appealing features including intense light absorption, excellent ambipolar charge mobility, and small exciton binding energy,[12-14] which justify their efficient performance in various cell structures.[3-6,15-17]

The most efficient perovskite solar cells have usually employed organic hole-transporting materials (HTMs), which play a key role in hole transportation and retardation of charge recombination.[18-20] So far, HTMs in perovskite solar cells mainly involve nitrogen-Containing donors,[18-25] such as 2,2',7,7'-tetrakis-(*N*,*N*-di-*p*-methoxyphenylamine)-9,9'-spiro-bifluorene (spiro-OMeTAD), poly-(triarylamine) (PTAA),[26] and so on. Due to the sp^3 hybridization of the nitrogen atom, the inherent triangular pyramid configuration leads to large intermolecular distances, thus suffer from low hole mobility, low conductivity, or both in their pristine form.[27,28] Therefore, ‘‘redox active’’ p-type dopants, such as Li-bis(trifluoromethanesulfonyl) imide (Li-TFSI), have been commonly adopted to increase their conductivity and thereby improve cell performance.[29-31] However, such dopants aggravated the cell performance degradation due to their deliquescent behaviour (Fig. S1†), and that the additional doping materials and doping process increase costs. Moreover, the p-type doping strategy requires strict optimization of doping conditions (e.g., solvent, dopants and doping concentrations). In this regard, developing dopant-free HTMs is important for efficient and durable inorganic-organic hybrid perovskite solar cells. To this end, one kind of the potential candidates is sulfur-containing conducting polymers due to their longer π-conjugations,[32,33] while those HTMs reported thus far display inferior performance in their pristine form for as-yet-unknown reasons, much less the difficult control of the regularity and high cost of them are adverse to the practical application. Another promising strategy to be considered reasonably is employing small molecular HTMs with planar configuration being conducive to strong intermolecular π-π stacking as appropriate candidates. To the best of our knowledge, however, application of such dopant-free HTMs in perovskite solar cells has been rarely reported to enable high performance.

In this study, we introduced an efficient dopant-free HTM for perovskite solar cells based on a small organic molecule, tetrathiafulvalene derivative TTF-1 (Scheme 1). The device achieved a power conversion efficiency of 11.03%, comparable to that of p-type doping spiro-OMeTAD based device. More importantly, the former device was three fold as stable as the latter in air at a relative humidity of 40%. The improved performance may be due to the following merits of tetrathiafulvalene (TTF). TTF has remarkable redox properties, with the first oxidation potential of 0.34 eV vs Ag/AgCl, corresponding to a highest occupied molecular orbital (HOMO) level of ~-5.0 eV vs vacuum level.[34] It matches well with the valence-band level of the organometal halide perovskite $CH_3NH_3PbI_3$ (~-5.4 eV vs vacuum level), ensuring sufficient driving force for hole transport from perovskite into their active layers. Owing to the strong electron donating ability of TTF moiety and feasible substitution at its 2,3,6,7 positions, it is easy to construct p-type semiconductors with efficient carrier mobility and to tune their molecular energy levels.[35-37] The inherent π-π stacking and strong S-S interactions between adjacent big rigidity conjugated units cause the hole conductivity of TTF derivatives to be efficient but result in their being less soluble or insoluble in most common solvents. Thus, the use of an expensive and time-consuming vacuum sublimation is required to fabricate their thin-film. The long alkyl chains in TTF-1 not only improve its solubility for solution processes, but also keep a certain intermolecular stacking because of the fastener-effect of the long alkyl chains. A highest hole mobility of TTF-1 thin film close to 0.1 $cm^2 \cdot V^{-1} \cdot s^{-1}$ has been reported.[38] For comparative analysis, two model HTMs poly(3-hexylthiophene) (P3HT) and spiro-OMeTAD were also studied (Scheme 1).

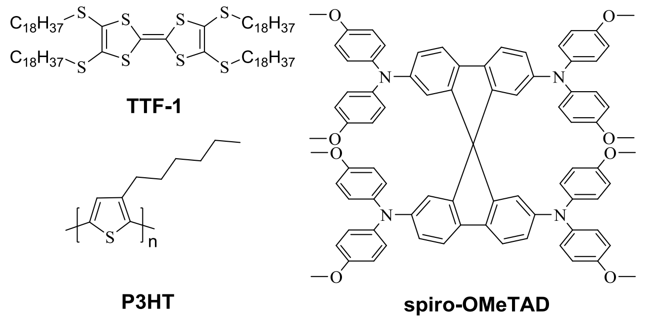

Scheme. 1 Molecular structures of **TTF-1**, **P3HT**, and **spiro-OMeTAD**.

UV-vis absorption spectra of TTF-1, P3HT, and spiro-OMeTAD in dichloromethane (DCM) and their thin films are shown in Fig. 1. In the DCM solutions, TTF-1 and spiro-OMeTAD show absorption bands in the UV region. In contrast, P3HT shows an absorption band in the visible region due to its longer π-conjugated backbone. In the thin-film states, both TTF-1 and P3HT exhibit approximately 100-nm red shifts compared to their absorption bands in solution. These results imply that there is a certain intermolecular π-π stacking in their thin-film states probably due to the strong S-S interaction, the fastener-effect of long alkyl chains, or both. However, similar absorption properties of spiro-OMeTAD were observed both in solution and in the thin-film state, indicating the poor π-π intermolecular interaction in its thin-film state.

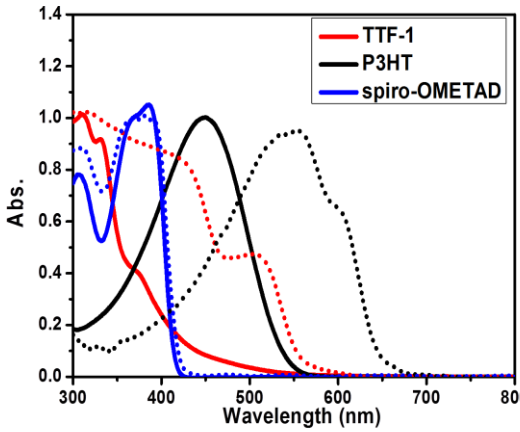

Fig. 1 Normalized absorption spectra of **TTF-1**, **P3HT**, and **spiro-OMeTAD** in DCM (solid line) and in the thin-film state (dotted line).

To investigate the potential application of TTF-1 as an HTM in hybrid perovskite solar cells, its electrochemical properties were studied by cyclic voltammetry in anhydrous DCM containing 0.1 M tetra-n-butylammonium hexafluorophosphate as a supporting electrolyte in a three-electrode system (Fig. S3†). A sulfur-containing analogue, P3HT, was also studied for comparative analysis. Both HTMs exhibit well-defined reversible oxidative waves. The highest occupied molecular orbital (HOMO) level of TTF-1 (-5.05 eV vs vacuum), was estimated from its ground-state oxidation potential in cyclic voltammograms, was slightly higher than that of P3HT (-5.20 eV vs vacuum). This result is in accord with the stronger electron-donating ability of the TTF core compared to the thiophene moiety. Unfortunately, the slight higher HOMO level of TTF-1 may result in lower photovoltage in the device, which will be discussed later. The optical band-gap energies (E_g) were estimate from the intersection between their normalized absorption and emission spectra in DCM (Fig. S2†). The lowest unoccupied molecular orbital (LUMO) energies were calculated by adding their E_g to the HOMO energies. An energy level diagram of the corresponding materials employed in perovskite solar cells is shown in Fig. 2.[19]

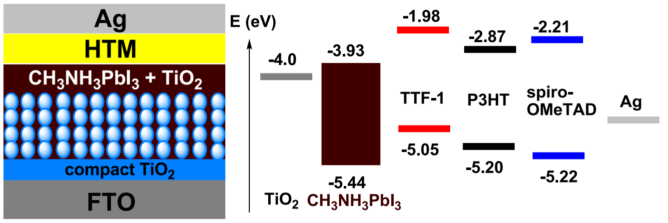

Fig. 2 Diagrammatic representation of photovoltaic device structure (left); Energy level diagram of the materials used in perovskite solar cells (right).

The preparation of the corresponding materials used in the fabrication of perovskite solar cells is detailed in Electronic Supplementary Information (ESI†). The solar cells were fabricated with a typical structure of FTO/ compact TiO_2/ mesoporous TiO_2/ perovskite/ HTM/ Ag (Fig. 2). The perovskite $CH_3NH_3PbI_3$ was deposited using a two-step sequential deposition method, which was first developed by Burschka et al.[5] The resulting perovskite films were coated with HTM via a solution process, both in their pristine form and in the presence of Li-TFSI and *tert*-butylpyridine (TBP). Details about the components and concentrations are provided in ESI†. It is noted that cells employing TTF-1 should be annealed at 65 °C in argon (20 °C below a solid-solid phase transition and 25 °C below the melting point according to the differential scanning calorimetry analysis, Fig. S6†) for 24 h to induce self-healing and diminish the density of defects existing at intergrain boundaries, thus enhance their photovoltaic performance. The cross-sectional structure of a representative device was investigated by scanning electron microscopy (Fig. S4c†). All devices employed the same conditions, except for the HTM, their light harvesting efficiencies were considered as the same reasonably (Fig. S7†).

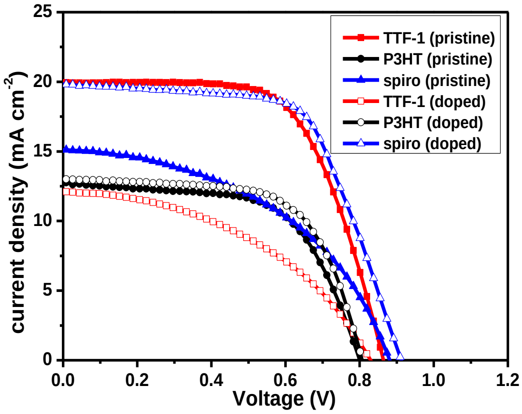

Fig. 3 Current–voltage curves of typical small-area (0.09 cm^2) perovskite solar cells based on **TTF-1**, **P3HT**, and **spiro-OMeTAD** in their pristine form or doped with Li-TFSI and TBP, respectively.

The photovoltaic characteristics of typical small-area perovskite solar cells (0.09 cm^2) based on three dopant-free HTMs (TTF-1, P3HT, and spiro-OMeTAD) were primarily evaluated under AM 1.5 G irradiation at 100 mW cm^{-2} (Fig. 3). The data are summarized in Table 1. The device based on dopant-free TTF-1 achieved an open-circuit voltage (V_{OC}) of 0.86 V, a short-circuit current (J_{SC}) of 19.9 mA cm^{-2}, a fill factor (FF) of 0.644, and an overall conversion efficiency (η) of 11.03%. As shown in Fig. S8†, the incident photon-to-current conversion efficiency spectrum (IPCE) of perovskite solar cells based on dopant-free TTF-1 ranged from UV region to 800 nm, which was match well with that of the UV-vis absorption spectrum of light harvester $CH_3NH_3PbI_3$ (Fig. S7†). However, devices based on dopant-free P3HT and dopant-free spiro-OMeTAD showed lower performances, the efficiencies being around 6%, mainly due to their lower J_{SC} and FF values, respectively (Table 1). The low FF (0.465) of perovskite solar cells based on dopant-free spiro-OMeTAD can partly be explained by their high series resistance (R_s, 158.2 Ω) due to the lower conductivity of spiro-OMeTAD in its pristine form. The fact that photocurrent of perovskite solar cells based on P3HT was lower than the photocurrents of cells based on small molecular HTMs, TTF-1 and spiro-OMeTAD, was probably due to the large molecular size of the P3HT polymer. The inferior pore-filling of P3HT resulted in a smaller interface between the perovskite and HTM, thus poor hole extraction and aggravated charge recombination.[18] Our results suggest that dopant-free HTMs using TTF-1 operate more efficiently than the well-known spiro-OMeTAD and P3HT for perovskite solar cells. We anticipated that employing dopant-free HTMs in perovskite solar cells would be synergistically beneficial in terms of cell durability by avoiding use of the deliquescent lithium salt (*vide infra*).

Table 1 Photovoltaic performance of perovskite solar cells based on HTMs in their pristine form or doped with Li-TFSI and TBP.[a]

HTM (form)	J_{SC} (mA cm^{-2})	V_{OC} (V)	FF	η (%)	R_s (Ω)
TTF-1 (pristine)	19.9	0.86	0.644	11.03	64.3
TTF-1 (doped)	12.1	0.83	0.439	4.41	162.4
P3HT (pristine)	12.8	0.80	0.607	6.22	72.1
P3HT (doped)	13.0	0.81	0.638	6.72	67.2
spiro-OMeTAD (pristine)	15.1	0.88	0.465	6.18	158.2
spiro-OMeTAD (doped)	19.8	0.91	0.631	11.4	70.6

[a] Measurements were performed under the following conditions: AM 1.5 G irradiation; cell area, 0.09 cm^2 determined by metal mask.

To compare with the common p-type doping strategy, perovskite solar cells based on these three HTMs with model additives (Li-TFSI and TBP) were also investigated. As summarized in Table 1, after p-type doping, the perovskite solar cells based on spiro-OMeTAD achieved higher J_{SC}, V_{OC}, and FF values, thus yielded a higher efficiency of 11.4%. The decrease in R_s from 158.2 to 70.6 Ω after p-type doping support the increased FF of the cells, thus primarily contributing the performance improvement. Such an effect of p-type dopants on sprio-OMeTAD for solid-state solar cells has been discussed in depth by Snaith[29,39] and Seok.[30] In contrast, perovskite solar cells based on p-type doping TTF-1 exhibit lower performance, especially in terms of FF and J_{SC}; the exact mechanism responsible for this abnormal phenomenon is unclear. The small distinction of photovoltaic performance in perovskite solar cells based on P3HT with or without p-type doping reveals that the lower performance of them seems to not originate from hole transport or conduction in HTMs, but probable being caused by the larger size and inferior interface in turn, and so forth.

The fact that both IPCE spectra and J_{SC} values obtained from the optimized perovskite solar cells based on dopant-free TTF-1 and p-type doping spiro-OMeTAD were almost the same, respectively (Fig. S8†). The results indicate that there is little difference in the charge collection of both. However, the photovoltage values in these two cases were somewhat different. The V_{OC} is relative to the difference between the conduction band of TiO_2 and the HOMO level of the hole conductor (theoretical photovoltage), and various interface losses in the photovoltaic system (charge recombination). According to the energy level diagram in Fig. 2, the theoretical photovoltage of perovskite solar cells based on TTF-1 is 170 mV lower than in the case of spiro-OMeTAD. However, a discrepancy of only 50 mV was observed between the V_{OC} values for the two cases. This result implies that TTF-1 may have an electron-blocking ability superior to that of spiro-OMeTAD and thus may be able to reduce the V_{OC} loss. While no systematic investigation was undertaken in the present communication. Whether the long alky chains have an effect on the retardation of charge recombination, electron blocking, or both should be further investigated in future research. Similar phenomena have been discussed in depth in dye-sensitized solar cells systems.[40]

For the advancement of practical perovskite solar cells, the cell durability is an important issue. Actually, there are many factors that influence the stability of perovskite solar cells, such as temperature, moisture and so on. In this study, we confirmed the expectation that using dopant-free HTMs is significant for the cell durability enhancement. As shown in Fig. 4, cells based on dopant-free TTF-1 without encapsulation does exhibit slightly and slowly degradation under ambient conditions at room temperature with a humidity of about 40%, which is more stable than cells based on common p-type doping spiro-OMeTAD under the same conditions. On the basis of the degradation time associated with a 20 % decrease of efficiency, we estimate the lifetime of cells based on dopant-free TTF-1 (~ 360 h) to be three times that of cells based on p-type doping spiro-OMeTAD (~ 120 h). The enhanced durability of perovskite solar cells based on dopant-free TTF-1 compared with cells based on p-type doping spiro-OMeTAD can be attributed mainly to avoiding the use of deliquescent additives. In addition, hydrophobic alkyl chains in TTF-1 molecules may also contribute to this improvement. Furthermore, a device based on dopant-free TTF-1 with a larger area (1.00 cm^2) was also prepared and evaluated under AM 1.5 G irradiation at 100 mW cm^{-2} (Fig. S9†). The J_{SC}, V_{OC}, and FF values (16.4 mA cm^{-2}, 0.83 V, and 0.594, respectively) were slightly lower than the corresponding values obtained with a small-area cell. An overall power conversion efficiency of 8.08% was obtained with this larger cell. These results highlight the potential application of organolead halide perovskite as a light harvester and TTF-1 as a dopant-free HTM in hybrid solar cells.

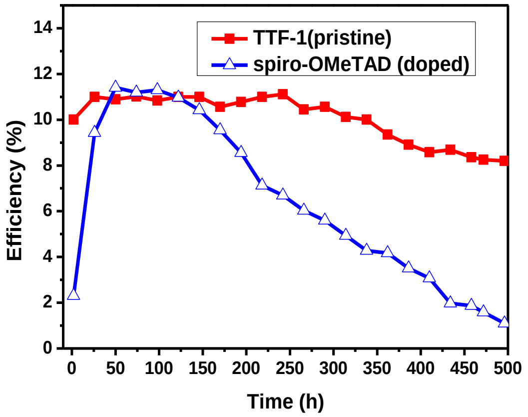

Fig. 4 Efficiency variation of optimized cells based on dopant-free **TTF-1** (pristine) and p-type doping **spiro-OMeTAD** (doped). Unencapsulated cells were stored in air at room temperature with a humidity of about 40% and were measured under illumination at AM 1.5 G.

In summary, TTF-1, a member of tetrathiafulvalene family, has been demonstrated for the first time to be a promising HTM candidate for perovskite solar cells without using lithium salts and TBP. To the best of our knowledge, this is the first case of perovskite solar cells employing dopant-free HTM based on tetrathiafulvalene derivative yielding an efficiency over 11%, which is comparable with that obtained using the well-known p-type doping spiro-OMeTAD; moreover, the stability of dopant-free TTF-1 based cells was greatly improved by 2 fold in air at a common relative humidity of 40%. The present results show that TTF-1 is superior to spiro-OMeTAD and P3HT as dopant-free HTMs in these hybrid solar cells. The fact that a module (1 cm × 1 cm) based on dopant-free TTF-1 yielded an efficiency over 8% highlights its potential application in perovskite solar cells. The feasibility of tailoring the structure and tuning the properties of TTF derivatives guarantee their bright future as dopant-free HTMs in perovskite solar cells. Further enhancement of efficiency could be realized by developing new tetrathiafulvalene derivatives with excellent electrical properties and proper oxidation potential with respect to the energy level of perovskite. Work on these and systematic investigation of the effect of long alkyl chains on cell performance and stability is now in progress.

Acknowledgements

This work was supported by the Core Research for Evolutional Science and Technology of the Japan Science and Technology Agency.

Notes and references

Photovoltaic Materials Unit, National Institute for Materials Science, Sengen 1-2-1, Tsukuba, Ibaraki 305-0047, Japan Fax:+81-29-859-2304; Tel: +81-29-859-2305; E-mail: HAN.Liyuan@nims.go.jp, YANG.Xudong@nims.go.jp

† Electronic Supplementary Information (ESI) available: Experimental methods, photovoltaic characteristics, cyclic voltammetry results, absorption spectrum of $CH_3NH_3PbI_3$, X-ray diffraction, scanning electron microscopy, and differential scanning calorimetry results. See DOI: 10.1039/c000000x/

1 A. Kojima, K. Teshima, Y. Shirai, T. Miyasaka, *J. Am. Chem. Soc.*, 2009, **131**, 6050.
2 M. M. Lee, J. Teuscher, T. Miyasaka, T. N. Murakami, H. J. Snaith, *Science*, 2012, **338**, 643.
3 H.-S. Kim, C.-R. Lee, J.-H. Im, K.-B. Lee, T. Moehl, A. Marchioro, S.-J. Moon, R. Humphry-Baker, J.-H. Yum, J. E. Moser, M. Grätzel, N.-G. Park, *Sci. Rep.*, 2012, **2**, 591.
4 M. Liu, M. B. Johnston, H. J. Snaith, *Nature*, 2013, **501**, 395.
5 J. Burschka, N. Pellet, S.-J. Moon, R. Humphry-Baker, P. Gao, M. K. Nazeeruddin, M. Grätzel, *Nature*, 2013, **499**, 316.
6 D. Liu, T. L. Kelly, *Nat. Photonics*, 2014, **8**, 133.
7 J. H. Noh, S. H. Im, J. H. Heo, T. N. Mandal, S. Il. Seok, *Nano Lett.*, 2013, **13**, 1764.
8 M. A. Green, K. Emery, Y. Hishikawa, W. Warta, E. D. Dunlop, *Prog. Photovoltaics*, 2014, **22**, 1.
9 S. Kazim, M. K. Nazeeruddin, M. Grätzel, S. Ahmad, *Angew. Chem. Int. Ed.*, 2014, **53**, 2.
10 Research Cell Efficiency Records published by NREL, 2014.
11 K. Wojciechowski, M. Saliba, T. Leijtens, A. Abatea, H. J. Snaith, *Energy Environ. Sci.*, 2014, **7**, 1142.

12 S. D. Stranks, G. E. Eperon, G. Grancini, C. Menelaou, M. J. P. Alcocer, T. Leijtens, L. M. Herz, A. Petrozza, H. J. Snaith, *Science*, 2013, **342**, 341.

13 G. Xing, N. Mathews, S. Sun, S. S. Lim, Y. M. Lam, M. Grätzel, S. Mhaisalkar, T. C. Sum, *Science*, 2013, **342**, 344.

14 C. Wehrenfennig, G. E. Eperon, M. B. Johnston, H. J. Snaith, L. M. Herz, *Adv. Mater.*, 2014, **26**, 1584.

15 L. Etgar, P. Gao, Z. Xue, Q. Peng, A. K. Chandiran, B. Liu, M. K. Nazeeruddin, M. Grätzel, *J. Am. Chem. Soc.*, 2012, **134**, 17396.

16 W. A. Laban, L. Etgar, *Energy Environ. Sci.*, 2013, **6**, 3249.

17 O. Malinkiewicz1, Aswani. Yella, Y. H. Lee, G. M. Espallargas, M. Grätzel, M. K. Nazeeruddin, H. J. Bolink, *Nat. Photonics*, 2014, **8**, 128.

18 D. Bi, L. Yang, G. Boschloo, A. Hagfeldt, E. M. J. Johansson, *J. Phys. Chem. Lett.*, 2013, **4**, 1532.

19 N. J. Jeon, J. Lee, J. H. Noh, M. K. Nazeeruddin, M. Grätzel, S. Il. Seok, *J. Am. Chem. Soc.*, 2013, **135**, 19087.

20 J. H. Heo, S. H. Im, J. H. Noh, T. N. Mandal, C.-S. Lim, J. A. Chang, Y. H. Lee, H.-j. Kim, A. Sarkar, M. K. Nazeeruddin, M. Grätzel, S. Il. Seok, *Nat. Photonics*, 2013, **7**, 486.

21 T. Krishnamoorthy, F. Kunwu, P. P. Boix, H. Li, T. M. Koh, W. L. Leong, S. Powar, A. Grimsdale, M. Grätzel, N. Mathews, S. G. Mhaisalkar, *J. Mater. Chem. A*, 2014, **2**, 6305.

22 H. Li, K. Fu, A. Hagfeldt, M. Grätzel, S. G. Mhaisalkar, A. C. Grimsdale, *Angew. Chem. Int. Ed.*, 2014, **53**, 4085.

23 J. Wang, S. Wang, X. Li, L. Zhu, Q. Meng, Y. Xiao, D. Li, *Chem. Commun.*, 2014, **50**, 5829.

24 N. J. Jeon, H. G. Lee, Y. C. Kim, J. Seo, J. H. Noh, J. Lee, S. Il. Seok, *J. Am. Chem. Soc.*, 2014, **136**, 7837.

25 S. Lv, L. Han, J. Xiao, L. Zhu, J. Shi, H. Wei, Y. Xu, J. Dong, X. Xu, D. Li, S. Wang, Y. Luo, Q. Meng, X. Li, *Chem. Commun.*, 2014, DOI: 10.1039/C4CC02211D.

26 S. Ryu, J. H. Noh, N. J. Jeon, Y. C. Kim, W. S. Yang, J. Seo, S. Il. Seok, *Energy Environ. Sci.*, 2014, DOI: 10.1039/C4EE00762J.

27 J. Burschka, A. Dualeh, F. Kessler, E. Baranoff, N. L. Cevey-Ha, C. Y. Yi, M. K. Nazeeruddin, M. Grätzel, *J. Am. Chem. Soc.*, 2011, **133**, 18042.

28 T. Leijtens, J. Lim, J. Teuscher, T. Park, H. J. Snaith, *Adv. Mater.*, 2013, **25**, 3227.

29 A. Abate, T. Leijtens, S. Pathak, J. Teuscher, R. Avolio, M. E. Errico, J. Kirkpatrik, J. M. Ball, P. Docampo, I. McPhersonc, H. J. Snaith, *Phys. Chem. Chem. Phys.*, 2013, **15**, 2572.

30 J. H. Noh, N. J. Jeon, Y. C. Choi, M. K. Nazeeruddin, M. Grätzel, S. Il. Seok, *J. Mater. Chem. A*, 2013, **1**, 11842.

31 H. Zhang, Y. Shi, F. Yan, L. Wang, K. Wang, Y. Xing, Q. Dong, T. Ma, *Chem. Commun.*, 2014, **50**, 5020.

32 B. Cai, Y. Xing, Z. Yang, W.-H. Zhang, J. Qiu, *Energy Environ. Sci.*, 2013, **6**, 1480.

33 Y. S. Kwon, J. Lim, H.-J. Yun, Y.-H. Kim, T. Park, *Energy Environ. Sci.*, 2014, **7**, 1454.

34 G. V. Tormos, M. G. Bakker, P. Wang, M. V. Lakshmikantham, M. P. Cava, R. M. Metzger, *J. Am. Chem. Soc.*, 1995, **117**, 8528.

35 M. Mas-Torrent, M. Durkut, P. Hadley, X. Ribas, C. Rovira, *J. Am. Chem. Soc.*, 2004, **126**, 984.

36 C. Rovira, *Chem. Rev.*, 2004, **104**, 5289.

37 I. Doi, E. Miyazaki, K. Takimiya, Y. Kunugi. *Chem. Mater.*, 2007, **19**, 5230.

38 P. Miskiewicz, M. Mas-Torrent, J. Jung, S. Kotarba, I. Glowacki, E. Gomar-Nadal, D. B. Amabilino, J. Veciana, B. Krause, D. Carbone, C. Rovira, J. Ulanski, *Chem. Mater.*, 2006, **18**, 4724.

39 A. Abate, D. R. Staff, D. J. Hollman, H. J. Snaith, A. B. Walker, *Phys. Chem. Chem. Phys.*, 2014, **16**, 1132.

40 Z. J. Ning, Y. Fu, H. Tian, *Energy Environ. Sci.*, 2010, **3**, 1170.